

ACCRETION AND THERMAL EVOLUTION OF IIAB AND IIIAB IRON METEORITE PARENT BODIES INFERRED FROM MN-CR CHRONOMETRY. A. Anand¹, J. Pape^{1,2}, M. Wille¹, K. Mezger¹ and B. Hofmann^{1,3}, ¹Institut für Geologie, Universität Bern, Baltzerstrasse 1+3, 3012 Bern, Switzerland (aryavart.anand@geo.unibe.ch), ²Institut für Planetologie, Universität Münster, Wilhelm-Klemm-Str. 10, 48149 Münster, Germany, ³Naturhistorisches Museum Bern, Bernastrasse 15, CH-3005, Bern, Switzerland.

Introduction: The IIAB and IIIAB iron meteorites belong to the category of “magmatic irons”, and are thought to sample the core of distinct parent bodies that experienced large-scale chemical fractionation, most notably metal-silicate separation. The time of metal core formation in the magmatic iron meteorite parent bodies provides a key time marker for the evolution of early formed planetesimals including the accretion and cooling history of the parent body. The timing and duration of such early Solar System processes, including accretion, differentiation and subsequent cooling, can be investigated using the short-lived ⁵³Mn-⁵³Cr chronometer ($t_{1/2} \approx 3.7$ Ma). Chromite (FeCr₂O₄) and daubréelite (FeCr₂S₄) are the two main carrier phases of Cr in IIAB and IIIAB iron meteorites. Both these minerals have low Mn/Cr ratios (≈ 0.01) and thus, preserve the Cr isotope composition of their growth environment at the time of isotopic closure, while the ingrowth of radiogenic ⁵³Cr from in-situ decay of ⁵³Mn is negligible. Model ages for chromite and daubréelite in IIAB and IIIAB iron meteorites can be obtained by comparing their Cr-isotopic composition with the Cr-isotope evolution of its assumed reservoir. In order to systematically resolve the ingrowth of ⁵³Cr over a time span of a very few Myrs, Cr isotope abundances need to be measured with high precision by TIMS. The present study reports chromite and daubréelite model ages for IIAB and IIIAB iron meteorites. The age data provides constraints on the accretion time and evolution of their parent bodies.

Methods: Two IIIAB (Cape York and Saint Aubin) and three IIAB (Sikhote Alin, Agoudal and NWA 11420) iron meteorite samples were analyzed in this study. The whole rock fragments were hand crushed using an agate mortar and treated in conc. aqua regia on a hot plate set to 90 °C for 48 hrs. to completely dissolve the metal-sulfide dominated matrix, leaving behind chromite particles as residue. In case of sample NWA 11420, a 16 g rock fragment was treated with conc. aqua regia on a hot plate set to 90 °C for 12 hrs. and the residue was further classified as magnetic and nonmagnetic depending on its magnetic behavior. Daubréelite grains were isolated in the non-magnetic portion and then handpicked. Chromite and daubréelite grains weighing 2-5 mg from all the samples were transferred in a 7 ml vials with 150-250 mg of Ammonium bifluoride (NH₄F·HF, Sigma-Aldrich, Trace

Metal grade) and completely digested following the protocol described in [1]. In summary, the sample and reagent mixture was thermalized in a convection oven set to 230 °C for 48 hrs. Upon cooling, the mixture was dried twice, first with 2 ml conc. HNO₃ and then with 1 ml conc. HNO₃ and 2 ml MilliQ® water. Purification of Cr from the dissolved samples follows a combination of three steps of cation-anion exchange chromatography adopted from [2]. The purified Cr was loaded onto outgassed single Re filaments with 1.4 µL alumina doped Si gel activator. The samples were analyzed by Thermo Scientific Triton Plus TIMS instrument at University of Bern. Each sample was measured on 10-12 filaments and isotope compositions are reported as parts per 10,000 deviations (ϵ -notation) from the mean value of the NIST SRM 979 Cr standard measured along with the samples in each session.

Model for $\epsilon^{53}\text{Cr}$ evolution in chondritic reservoir. The model assumes that chondrites represent an isotopically homogeneous reservoir for Cr and Mn that evolved with a distinct Mn/Cr ratio after primordial nebular Mn/Cr fractionation and isolation of the precursor material of chondrites, terrestrial planets and differentiated planetesimals (parent bodies of iron meteorites) [3]. The evolution of the ⁵³Cr/⁵²Cr isotope composition of the chondritic reservoir through time can be expressed as (Eq. 1):

$$(^{53}\text{Cr}/^{52}\text{Cr})_p = (^{53}\text{Cr}/^{52}\text{Cr})_i + (k)(^{53}\text{Mn}/^{55}\text{Mn})_i \times (1 - e^{-\lambda t})$$

where p refers to the present values, i refers to the initial values and λ denotes the ⁵³Mn decay constant. The ⁵⁵Mn/⁵²Cr of the reservoir is denoted by k ; and t represents the time elapsed since the start of the solar system, which is equated with the time of formation of CAIs. Eq. 1 describes the evolution of ⁵³Cr/⁵²Cr with time for the chondritic reservoir and can be used to derive model ages for a meteorite sample by measuring the Cr isotopic composition of its chromite/daubréelite fraction only.

Results: $\epsilon^{53}\text{Cr}$ and $\epsilon^{54}\text{Cr}$ of chromite/daubréelite fractions determined in all the samples are listed in Table 1. Due to significantly high radiogenic $\epsilon^{53}\text{Cr}$ and low Fe/Cr ratios in chromite/daubréelite, cosmogenic contributions are negligible and hence no correction for spallogenic Cr is required [4]. Model ages are calculated

ed relative to the CAI formation age of 4567.11 ± 0.16 Ma [5] using Eq.1 and $\epsilon^{53}\text{Cr}$ of the samples assuming solar system initial $\epsilon^{53}\text{Cr} = -0.23$, CI chondritic $^{55}\text{Mn}/^{52}\text{Cr} = 0.71$ and a canonical $^{53}\text{Mn}/^{55}\text{Mn} = 6.28 \times 10^{-6}$ [3]. The ages are plotted on a chondritic $\epsilon^{53}\text{Cr}$ evolution diagram as shown in Fig. 1. The model ages range from 0.0 ± 0.4 to 0.4 ± 0.7 Ma for IIAB and -0.4 ± 0.4 to 0.9 ± 0.5 Ma for IIIAB samples.

Table 1. Cr isotopic composition of samples.

Sample	Group/Fraction	$\epsilon^{53}\text{Cr}$	2SE	$\epsilon^{54}\text{Cr}$	2SE
Agoudal	IIAB/Chromite	-0.21	0.02	-0.78	0.06
Sikhote Alin	IIAB/Chromite	-0.23	0.03	-0.92	0.05
NWA 11420	IIAB/Daubreelite	-0.20	0.04	-0.77	0.06
Saint Aubin	IIIAB/Chromite	-0.26	0.03	-0.78	0.06
Cape York	IIIAB/Chromite	-0.17	0.03	-0.73	0.06

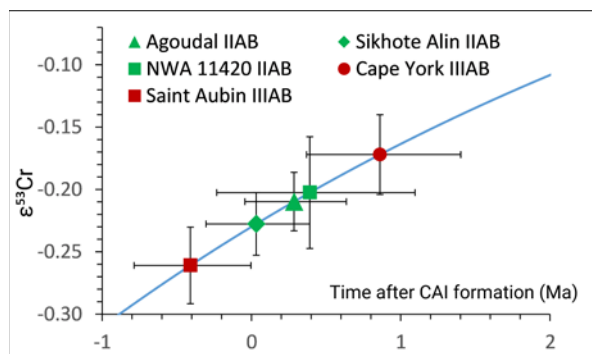


Fig. 1. The model ages are plotted on a curve representing the $\epsilon^{53}\text{Cr}$ evolution of the chondritic reservoir through time. Uncertainties on the model ages are determined using uncertainties on the $\epsilon^{53}\text{Cr}$ values of the samples.

Discussion: The model ages reported in the present study are determined using initial $\epsilon^{53}\text{Cr} = -0.23$ and a canonical $^{53}\text{Mn}/^{55}\text{Mn} = 6.28 \times 10^{-6}$ [3]. However, different studies have reported resolvable variations in the solar system initial $\epsilon^{53}\text{Cr}$ and $^{53}\text{Mn}/^{55}\text{Mn}$ values. Using the solar system initial $\epsilon^{53}\text{Cr} = -0.177$ and canonical $^{53}\text{Mn}/^{55}\text{Mn} = 6.8 \times 10^{-6}$ reported by [6] results in model ages ranging from of -0.6 to -0.3 for IIAB and -1.0 to -0.5 Ma for IIIAB samples. These ages predate the CAI formation age contradictory to the standard solar system model where the CAI are the earliest formed solid objects [7] and also, do not correlate with other chronometers (Hf-W, Pd-Ag). Altogether, the initial $\epsilon^{53}\text{Cr}$ and ^{53}Mn abundances reported in [3] produce a more consistent data set for Mn-Cr ages and hence adopted in the present study.

Mn-Cr chromite/daubreelite model ages provide firm constraints on the timing of silicate-metal segregation in IIAB and IIIAB iron meteorite parent bodies.

The anchoring of the Mn-Cr model ages to the core formation event is based on the assumption that the core formed in a single event by metal-silicate separation inducing a strong chemical fractionation of Mn from more siderophile Cr (under certain conditions [8]). The $\epsilon^{53}\text{Cr}$ from the studied samples are within analytical uncertainty indistinguishable from the solar system initial $\epsilon^{53}\text{Cr}$, implying that these iron meteorites are as old as refractory CAI inclusions.

The Mn-Cr model ages of IIAB iron meteorites determined in the present study are in good agreement with the Hf-W core formation ages of 0.7 ± 0.3 Ma after CAI formation [9]. Mn-Cr model age of 0.9 ± 0.5 for sample Cape York agrees with the mean Hf-W core formation age of 1.2 ± 0.3 Ma for IIIAB iron meteorites [9]. Mn-Cr systematics in phosphates (sarcopside, graffonite, beusite, galileiite, and johnsomervilleite) in IIIAB iron meteorites were investigated by [10] and a thermal history at an early stage (<10 Ma after CAI formation) was determined. Coeval to the Hf-W systematics in IIIAB samples, Mn-Cr chronological data can be successfully fitted to this simple cooling history. Matthes M. et al. [11] reported Pd-Ag data for metal and troilite samples from the IIIAB iron Cape York and incorporated it in the cooling model showing that the IIIAB core was completely solidified at 2.6 ± 1.3 Ma.

The Mn-Cr model ages suggest that the core formation in IIAB and IIIAB iron meteorites occurred ≤ 1.5 Myr after the CAI formation and predates the formation of chondrules and the accretion of the chondrite parent bodies [12, 13]. The early planetary accretion and differentiation of the parent bodies of IIAB and IIIAB iron meteorites was sufficiently fast and ^{26}Al -decay was an effective heat source.

Acknowledgments: We appreciate the support through ‘Swiss Government Excellence Scholarship (2018.0371)’ and NCCR PlanetS supported by the Swiss National Science Foundation grant nr. 51NF40-141881.

References: [1] O'Hara M. et al. (2017) *Chem. Geo.* 466, 341-351. [2] Schoenberg R. et al. (2016) *GCA* 183, 14-30. [3] Trinquier A. et al. (2008) *GCA* 72, 5146-5163. [4] Liu J. et al. (2019) *GCA* 251, 73-86. [5] Amelin Y. et al. (2006) *Lunar Planet. Sci. Conf. XXXIV*, p. 1970. [6] Göpel C. et al. (2015) *GCA* 156, 1-24. [7] Scherstén A. et al. (2006) *EPSL* 241, 530-542. [8] Mann U. et al. *GCA* 73, 7360-7386. [9] Kruijer T. S. et al. (2014) *Science* 344-6188, 1150-1154. [10] Sugiura N. and Hoshino H. (2003) *Meteorit. Planet. Sci.* 38, 117-143. [11] Matthes M. et al. (2020) *GCA* 285, 193-206. [12] Pape J. et al. (2019) *GCA* 244, 416-436. [13] Pape J. et al. (2021) *GCA* 292, 499-517.